The effect of cantori on transport in chaotic magnetic fields

Stuart Hudson

Cantori are the invariant sets remaining after destruction of the KAM surfaces and create partial barriers to transport in chaotic fields.

This talk shall ..

1) give an explicit construction of cantori for magnetic fields,

2) give some review of cantori properties,

3) show that cantori affect advective-diffusive transport,

and 4) suggest "ghost coordinates" for chaotic fields . . .

Ideally the magnetic field is integrable, but non-axisymmetry destroys integrability.

- For 2-D (axisymmetric) systems, field lines lie on nested toroidal flux surfaces
  - rational surfaces : a continuous family of periodic orbits
  - irrational surfaces : closure of single irrational curve
- Stellarators are intrinsically 3-D (non-axisymmetric), and therefore chaotic . .
  - though they are designed to be as close to integrable as possible
- . . and some flux surfaces are destroyed.
  - the O and X periodic orbits form robust invariant periodic skeleton for chaos
  - the irrational <u>*curves*</u> survive, though not necessarily the irrational <u>*surfaces*</u>
  - KAM : sufficiently irrational surfaces survive sufficiently small perturbation
    - *[Kolmogorov 1954, Arnol'd 1963, Moser 1962]*
  - Greene : existence of KAM surfaces determined by stability of nearby periodic orbits *[Greene, 1979]*
- Cantorus : remnant invariant irrational set; KAM surface with gaps
    - *[Percival 1979; Aubry 1983; Mather 1982; MacKay . . .]*
  - *cantori play the dominant role in restricting transport in irregular regions*

Cantori restrict transport in chaotic regions

KAM torus
(complete barrier)

cantor+torus=cantorus
(partial barrier)

- *cantori are leaky, but can severely restrict transport (depending on degree of destruction)*

e.g. Poincare Plot

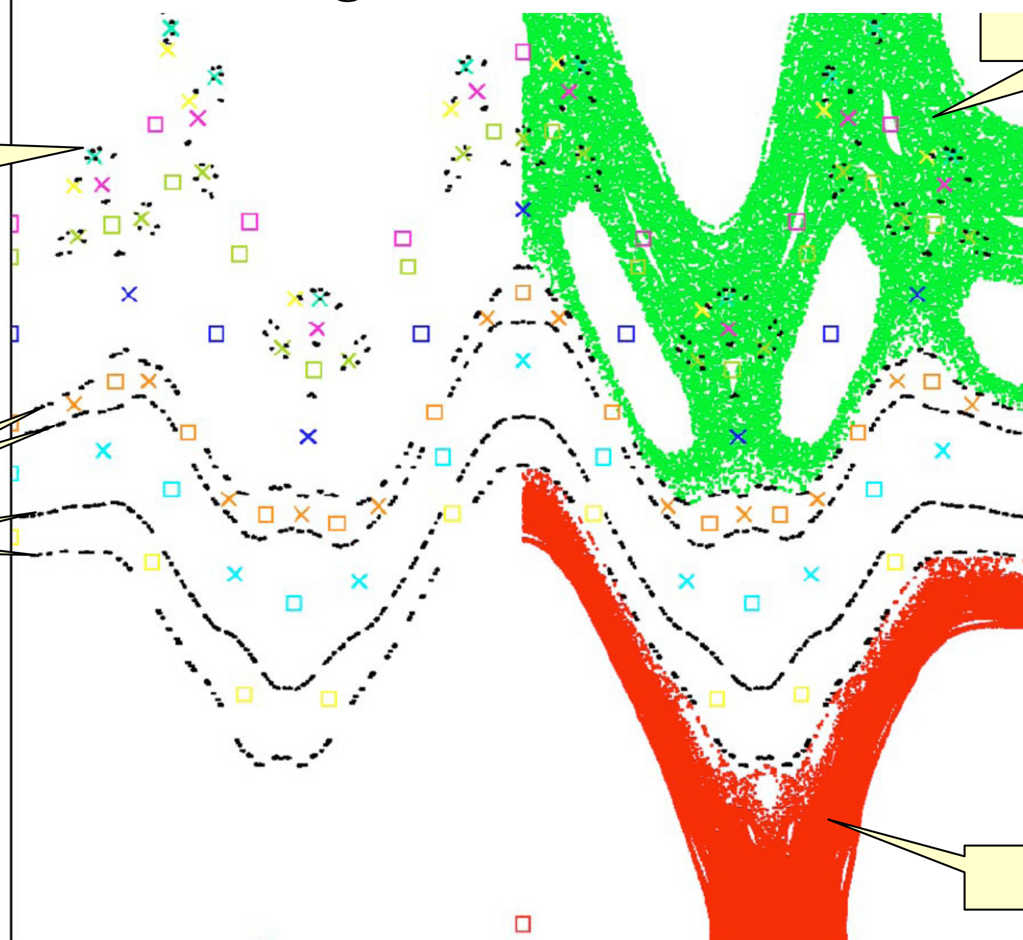

10^5 iterations

super critical cantori
(black dots)

connected chaos

(no KAM)

cantori restrict transport

near critical cantori

10^5 iterations

Cantori are identified by their (irrational) transform, approximated by periodic orbits.

Irrationals, and approximating rationals, conveniently expressed using continued fractions

Every irrational can be expressed $\iota = [a_o, a_1, a_2, ..] = a_0 + \cfrac{1}{a_1 + \cfrac{1}{a_2 + ..}}$; e.g. [0,2,1,1,1,..]=0.3820..

The convergents $p_n / q_n = [a_o, a_1, a_2, .., a_n]$ form a sequence of consecutively better approximates.

e.g.

[0,2,1,1]	$= 2/5$	$= 0.4000$
[0,2,1,1,1]	$= 3/8$	$= 0.3750$
[0,2,1,1,1,1]	$= 5/13$	$= 0.3846..$
[0,2,1,1,1,1,1]	$= 8/21$	$= 0.3810..$
[0,2,1,1,1,1,1,1]	$= 13/34$	$= 0.3824..$
[0,2,1,1,1,1,1,1,1]	$= 21/55$	$= 0.3818..$
[0,2,1,1,1,1,1,1,1,1]	$= 34/89$	$= 0.3820..$

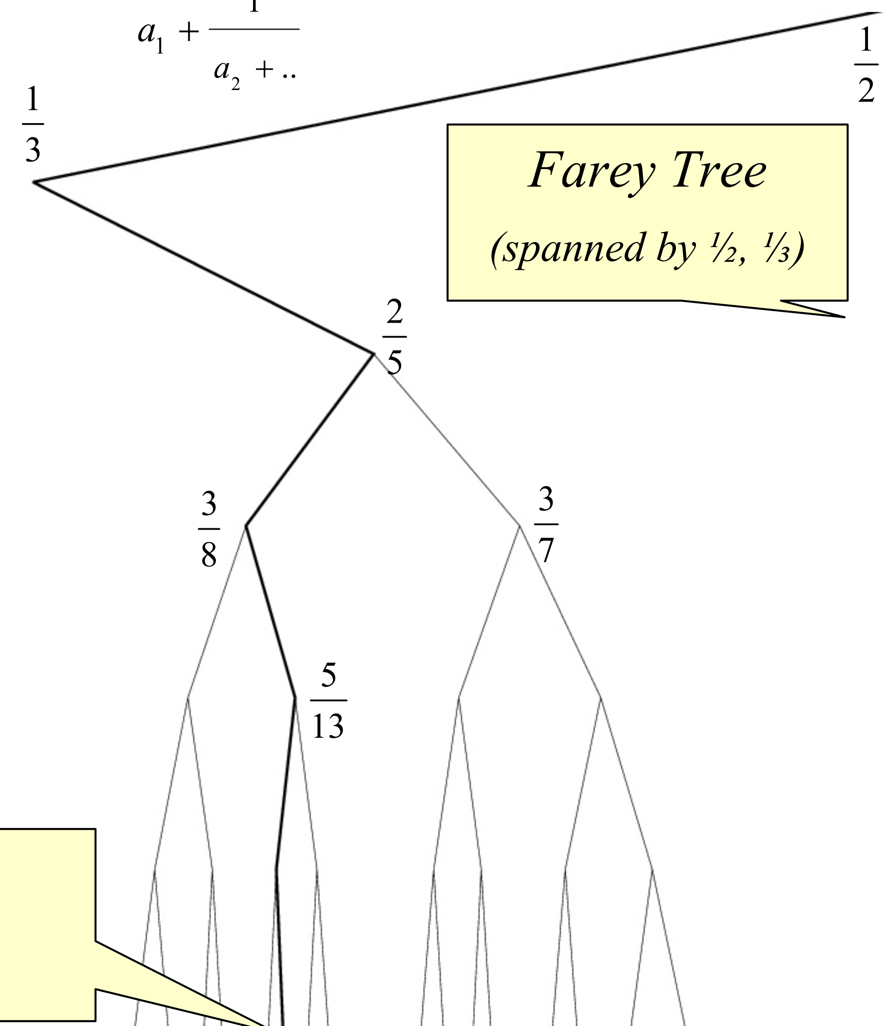

- *tails of 1,1,. = noble irrationals = alternating path;*
- *noble irrational KAM surfaces most robust;*
- *noble irrational cantori most important barriers;*

Outline of Talk

- Construction of cantori for magnetic field (Hamiltonian) flow
  - cantori approximated by (high-order) unstable periodic orbits
  - need to construct high-order periodic orbits, in chaotic regions, for continuous time magnetic field line flow (rather than discrete time mapping)
  - Lagrangian variational methods are robust, efficient, and field-line-flux across cantori easily quantified
- Investigation of effect of cantori on *diffusive* Hamiltonian flow
  - the advection-diffusion equation, with a chaotic flow, a discrete-time model, is solved numerically
  - graphical evidence is given that cantori (and the unstable manifold) have an important impact on the steady state distribution
- Describe ghost coordinates for chaotic fields
  - ghost curves are curves that connect the stable & unstable periodic orbits
  - these possibly may provide a convenient framework for understanding chaos . .

Magnetic field lines are determined from Lagrangian variational principles

Magnetic field lines, $\mathbf{B} = \nabla \times \mathbf{A}$, are stationary curves C of the action integral $S = \int_C \mathbf{A.dl}$,

$\mathbf{A} = \psi \nabla \theta - \chi \nabla \phi$ and $\chi(\psi,\theta,\phi) = \frac{1}{2}\psi^2 + \sum \chi_{m,n}(\psi)\cos(m\theta - n\phi)$.

Setting $\delta S = 0$ gives the field lines $\dot{\theta} = \partial_\psi \chi = B^\theta / B^\phi$, $\dot{\psi} = -\partial_\theta \chi = B^\psi / B^\phi$

Periodic orbits can be located by

1) field line following;

sensitive to exponential increase of integration error

2) adjusting a *trial curve* to find an extremum of S.

robust, efficient; need to specify trial curve

The simplest representation of a trial curve is piecewise-linear

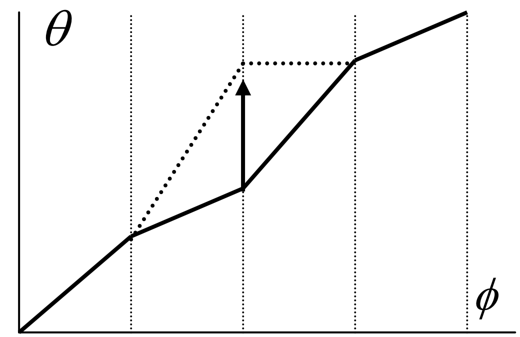

Trial Curve $\theta(\phi)$, $\psi = \dot{\theta}(\phi)$

Linear segment $\phi \in [\phi_i, \phi_{i+1}]$, $\theta = \theta_i + \psi_i(\phi - \phi_i)$, $\psi_{\mathrm{i}} = (\theta_{i+1} - \theta_i)/\Delta\phi$

Action integral integrated piecewise analytically

Action $S = \sum_i S_i(\theta_i, \theta_{i+1})$; $S_i = \int_{\phi_i}^{\phi_{i+1}} (\psi\dot{\theta} - \chi)\, d\phi = \frac{1}{2}\psi_i^2 + \sum_{m,n} \chi_{m,n}(\psi_i) \left[\frac{\sin(m\theta - n\phi)}{m\dot{\theta} - n} \right]_{\phi_i}^{\phi_{i+1}}$

Action Gradient:

To find extremal curves $\partial_i S = \partial_2 S_{i-1}(\theta_{i-1}, \theta_i) + \partial_1 S_i(\theta_i, \theta_{i+1}) = 0$, use Newton's method.

(periodic orbit constraint $\phi_0 = 0$, $\phi_N = 2\pi q$, $\theta_N = \theta_0 + 2\pi p$)

$$\begin{pmatrix} \delta\, \partial_0 S \\ \delta\, \partial_1 S \\ . \\ . \\ \delta\, \partial_{N\text{-}1} S \end{pmatrix} = \begin{pmatrix} \partial^2_{0,0} S & \partial^2_{0,1} S & 0 & 0 & \partial^2_{0,N-1} S \\ \partial^2_{1,0} S & \partial^2_{1,1} S & \partial^2_{1,2} S & 0 & 0 \\ 0 & . & . & . & 0 \\ 0 & 0 & . & . & . \\ \partial^2_{N-1,0} S & 0 & 0 & \partial^2_{N-1,N-2} S & \partial^2_{N-1,N-1} S \end{pmatrix} \begin{pmatrix} \delta\theta_0 \\ \delta\theta_1 \\ . \\ . \\ \delta\theta_{N-1} \end{pmatrix}$$

Hessian cyclic tridiagonal;
easily inverted O(N);
initial guess by tracking;
2nd order convergence;

if θ_0 constrained,
Hessian is tridiagonal

Unstable periodic orbits are action *minimizing* curves; stable periodic orbits are action *minimax* curves

- Cantori are approximated by action minimizing orbits
- Flux across island $\Phi_{p/q}$ is difference in action

$$\int_{Surface} \mathbf{B.n}\, ds = \int_{O\ curve} \mathbf{A.dl} - \int_{X\ curve} \mathbf{A.dl}$$

- Ghost surfaces are constructed by sliding a trial curve down the gradient flow, from the minimax to the minimum

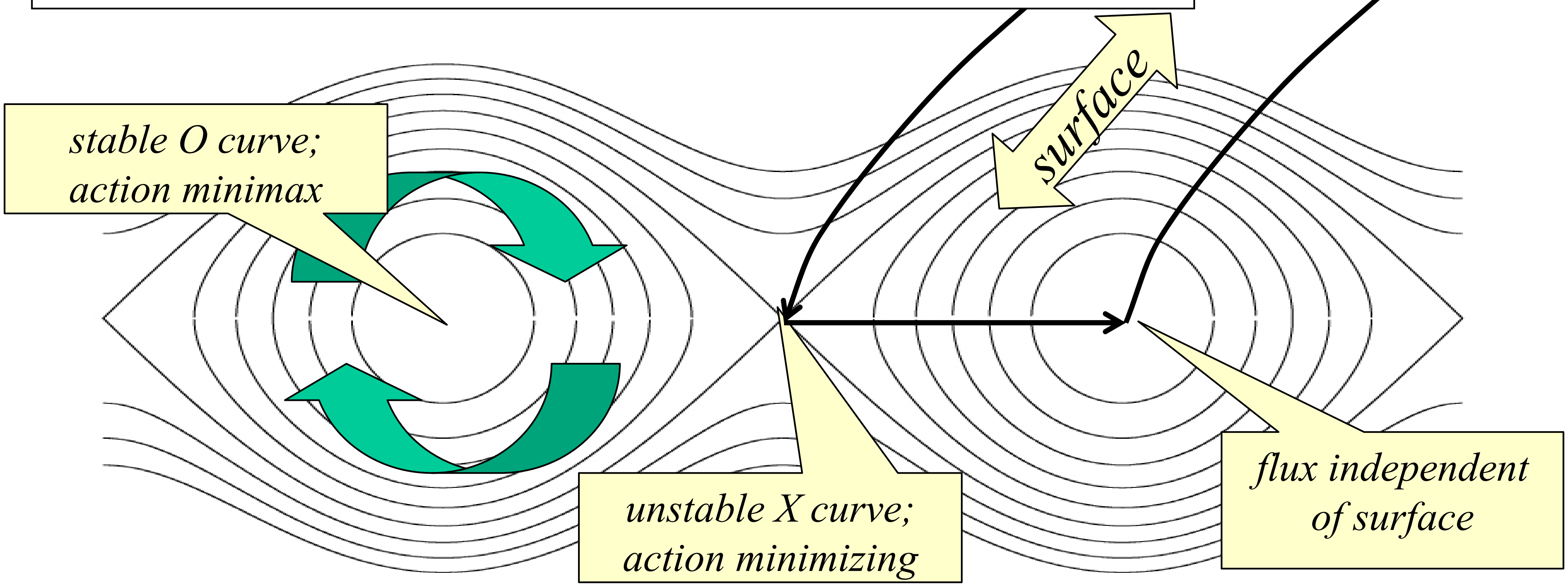

Analysis of chaotic magnetic field; construction of critical function, flux Farey tree

- Field line Hamiltonian $\chi = \psi^2/2 - k\left[\cos(2\theta-\phi)+\cos(3\theta-2\phi)\right]$;
- for non-zero k, islands form at $\iota = 1/2$ and $\iota = 2/3$, and all rational surfaces between;
- as k is increased, islands grow, overlap, and destroy enclosed KAM surfaces;
- the most irrational surfaces are most robust, most irrational cantori have minimal flux;

Critical Function

(application of Greene's residue criterion)

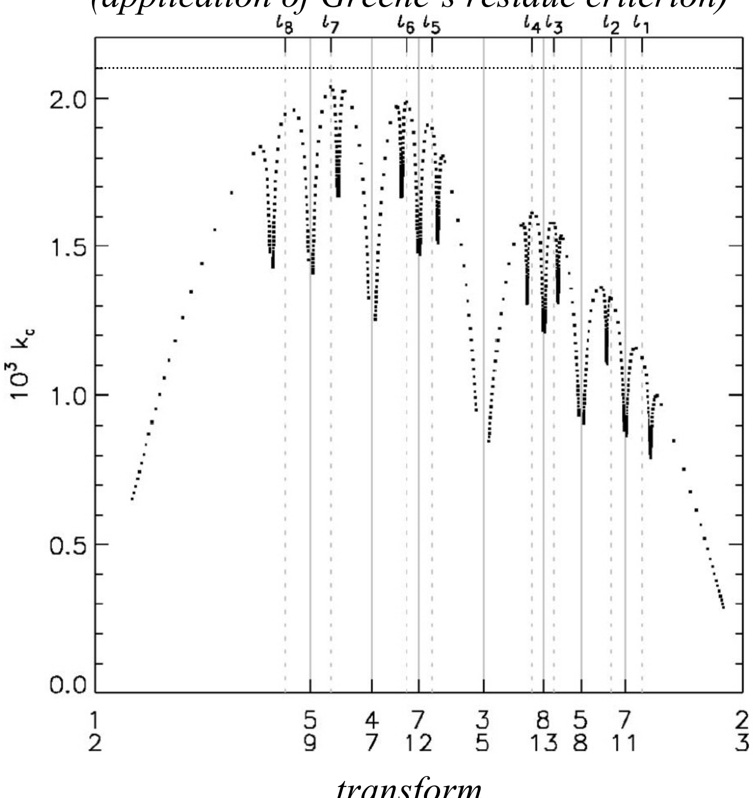

Flux Farey Tree

(for case $k=2.1\times10^{-3}$)

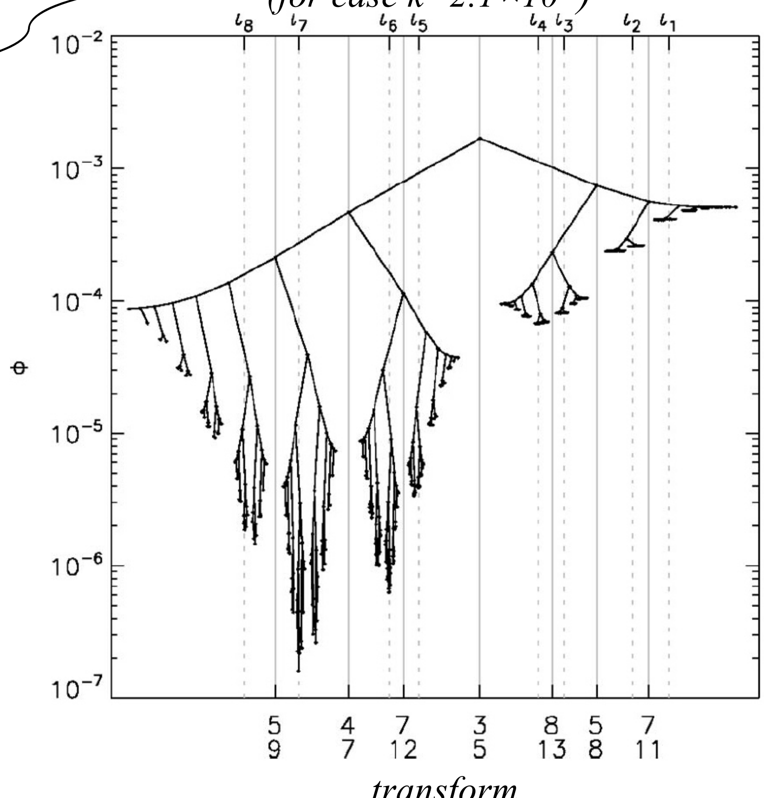

The Lagrangian variational approach provides an efficient, robust method of constructing high-order periodic orbits ≈ cantori

periodic orbits, with periodicity ~ 10^5, are located, even in strongly chaotic regions, for continuous time flows

$cont.fraction$	ι	p/q	k_c	$\Phi_{k=2.1}$
$[0,1,1,1,3,1,1^\infty]$	0.64..	$21282/33215$	1.1..	4.2×10^{-4}
$[0,1,1,1,2,1,1^\infty]$	0.63..	$16114/25463$	1.3..	2.6×10^{-4}
$[0,1,1,1,1,1,1^\infty]$	0.62..	$10946/17711$	1.6..	8.2×10^{-5}
$[0,1,1,1,1,2,1^\infty]$	0.61..	$15737/25696$	1.6..	6.8×10^{-5}
$[0,1,1,2,2,1,1^\infty]$	0.59..	$22879/38933$	1.9..	3.9×10^{-6}
$[0,1,1,2,1,1,1^\infty]$	0.58..	$15127/26073$	1.9..	6.1×10^{-7}
$[0,1,1,3,1,1,1^\infty]$	0.56..	$19308/34435$	2.0..	9.0×10^{-8}
$[0,1,1,4,1,1,1^\infty]$	0.55..	$23489/42797$	1.9..	1.8×10^{-6}

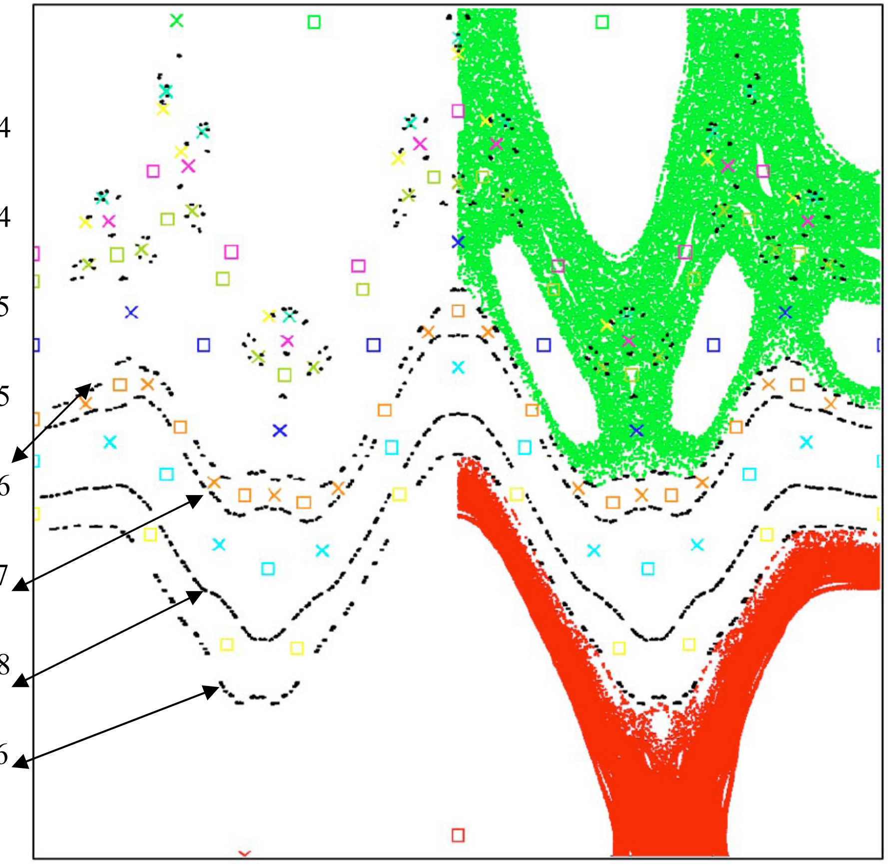

Higher periodic orbits approximate the cantori; the gap structure becomes clear.

$k < k_c$, KAM surface exists
high-order periodic orbits tend to fill curve

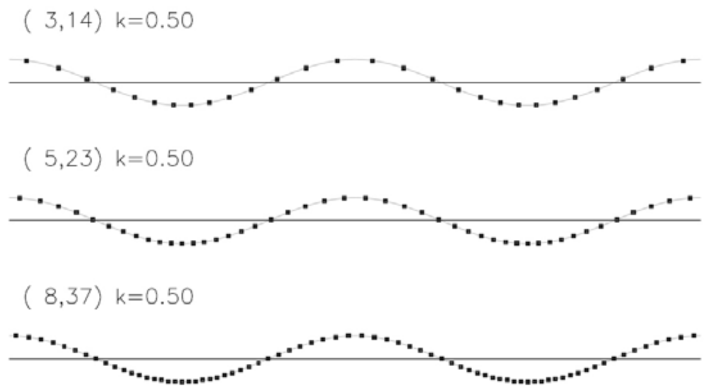

$k > k_c$, KAM surface destroyed
high-order periodic show gaps

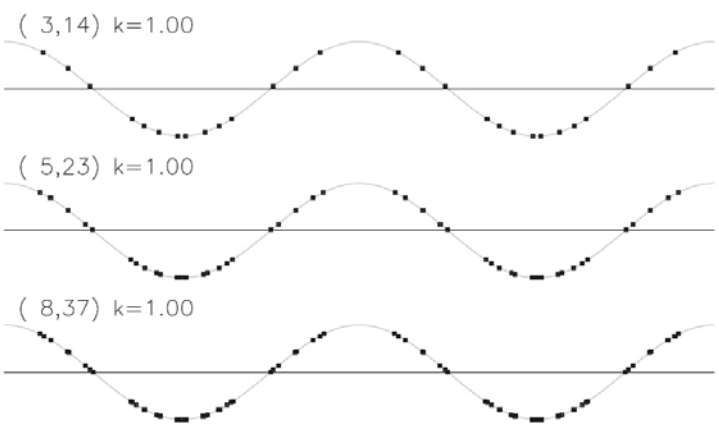

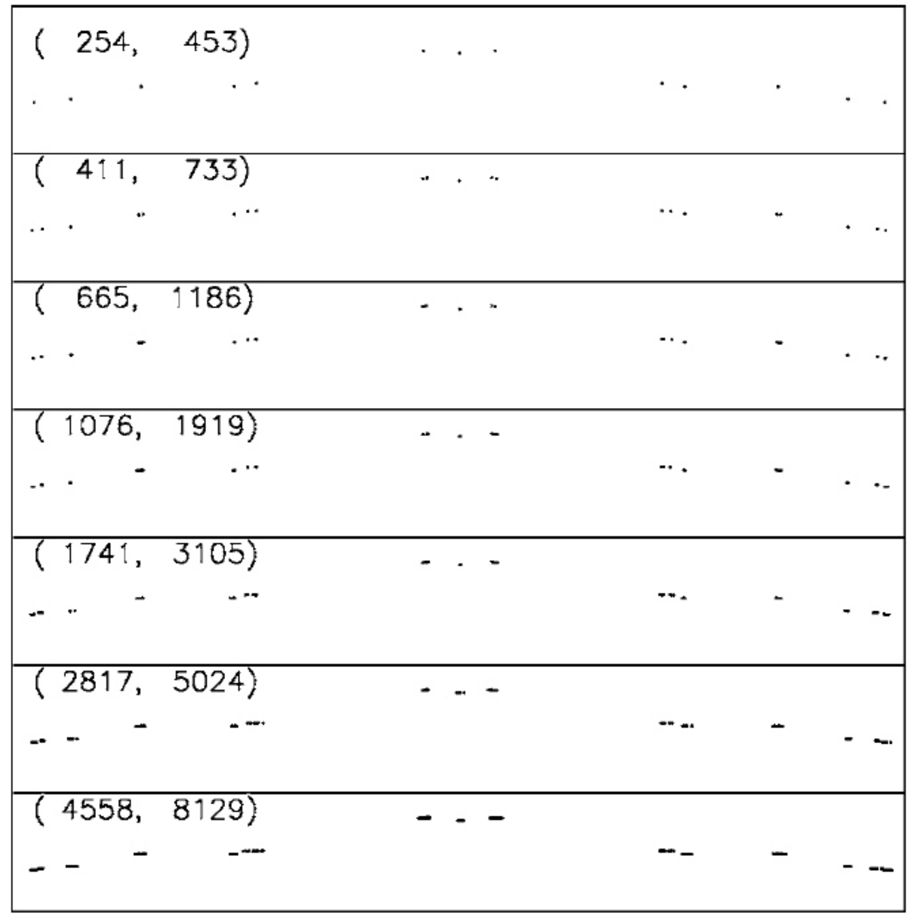

FIG. 5. Convergent minimizing-periodic orbits to the $[0,1,1,3,1^{\infty}]$ cantori, for the perturbation $k=2.10\times10^{-3}$. The horizontal θ range and vertical ψ range for each plot are [3.1315927, 3.1515927] and [0.5863, 0.5867], respectively.

The flux across a cantorus is given as the limit of the flux across the convergents

As the rational p_j/q_j approximation approaches the irrational ι,

the flux across an island chain approaches the flux across the cantorus

$\Phi_{p_j/q_j} \to \Phi_\iota$ as $p_j/q_j \to \iota$

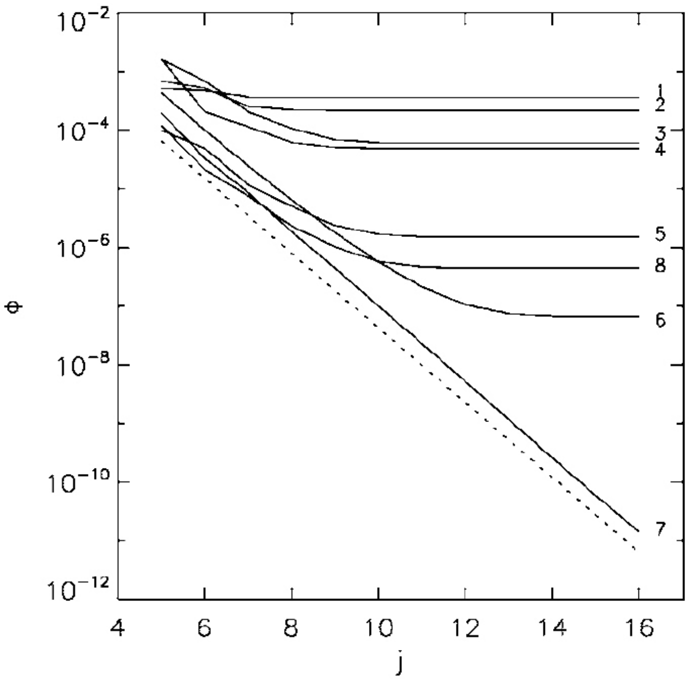

super critical : flux approaches non-zero value

$\Phi \sim \Delta\Phi + C\lambda^{-q_j}$

expressions from MacKay for nobles in std. map.

$\Phi \sim C\xi^{-j}$

near critical : flux across cantorus $\rightarrow$ zero

FIG. 4. Flux Φ_{p_j/q_j} against degree of convergent approximation j for each of the selected cantori, for $k=2.04\times10^{-3}$. The dashed line satisfies $\Phi=C\xi^j$ for $\xi=4.339$.

Piecewise linear approximation gives 2nd order error

The piecewise linear representation works well;

this is because the magnetic field lines are locally very smooth, being dominated by the strong toroidal field

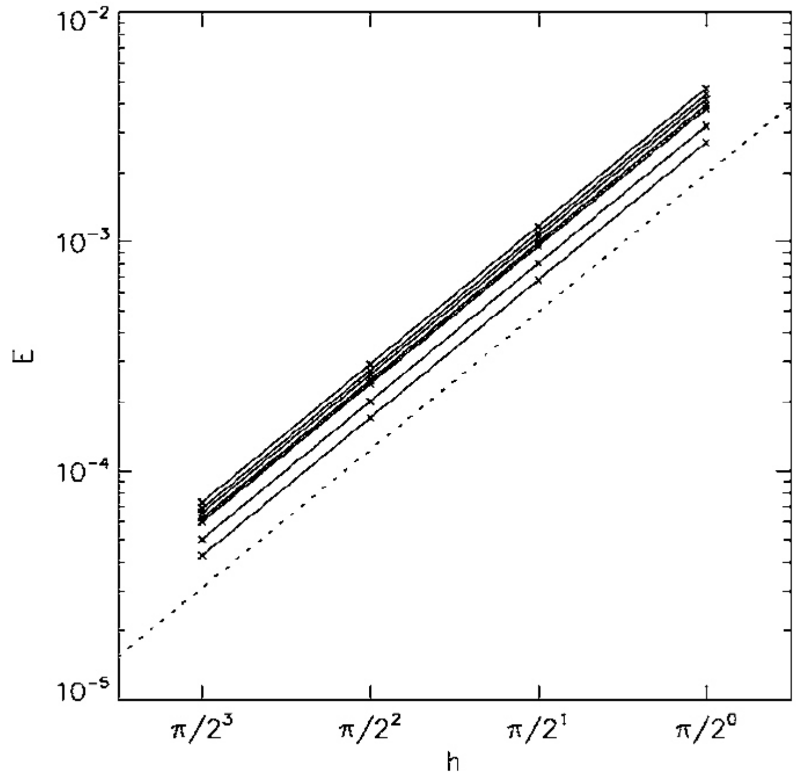

FIG. 6. Piecewise-linear approximation error against grid resolution. The dashed line has a gradient equal to 2.

Part I : Construction of cantori for flows : Summary

- Using the variational formulation, and piecewise-linear representation, cantori (high-order periodic orbits) are efficiently, and robustly, constructed for flows
  - previously, cantori had only been calculated for maps (eg. standard map)
  - periodic orbits, with periodicity ~ 10^4, calculated for chaotic fields (could probabaly be increased with some computational care)
  - robustly here means immune to Lyapunov exponentiation of error
- The *'flow'*-cantori share essential features of *'discrete'*-cantori
  - in particular, expressions for the flux across noble cantori are confirmed
- Cantori probably play an important role in chaotic transport
  - cantori are clearly dominant restriction to Hamiltonian transport
  - the remainder of this talk shall consider Hamiltonian+diffusive transport
- .

Now, moving on to Part II of this presentation, do cantori play an important role in *diffusive* Hamiltonian systems ?

Consider the advection-diffusion equation, $\partial_t T + v.\nabla T = D\nabla^2 T$,

with $\nabla \cdot v = 0$, and small diffusion constant, D.

$$\begin{pmatrix} x' \\ y' \end{pmatrix} = \begin{pmatrix} x + y - k\sin(2\pi x)/2\pi \\ y - k\sin(2\pi x)/2\pi \end{pmatrix}$$

Advection : continuous-time flow $\rightarrow$ discrete-time map (3D $\rightarrow$ 2D, reduces computational burden)

Diffusion : implicit curvilinear-coordinate (α, s) : $\nabla^2 T = \sqrt{g}^{-1}\left[\partial_\alpha\left(\sqrt{g}T^\alpha\right) + \partial_s\left(\sqrt{g}T^s\right)\right]$

symmetric finite-difference method : $T_\alpha\big|_{i+1/2,j+1/2} = \left(T_{i+1,j+1} + T_{i+1,j} - T_{i,j+1} - T_{i,j}\right)\big/ 2h_\alpha$

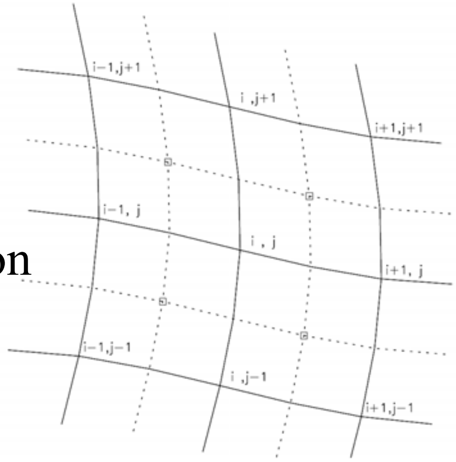

Steady state : advection balances diffusion

$\mathcal{L}_A T + \mathcal{B}_A = \mathcal{L}_D T + \mathcal{B}_D$

$L_D - L_A$ inverted using BiCGStab

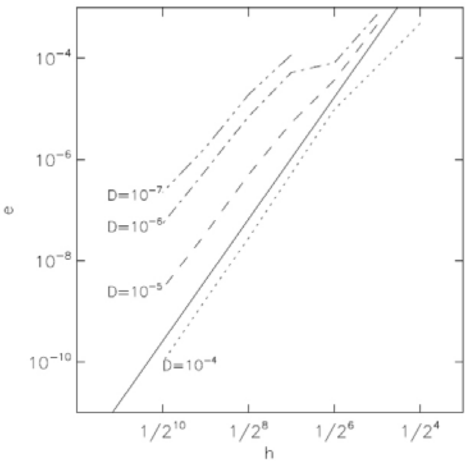

FIG. 6: Error scaling for various D, for $k = 0.95$. The solid line satisifes $e \sim h^4$.

Diffusion scale length $\Delta x = \sqrt{2D}$ $\leftarrow$ for small D require fine grid ($\sim 2^{11}$ in each dimension)

The 2D advection-diffusion equation is solved in a chaotic layer surrounding an island chain

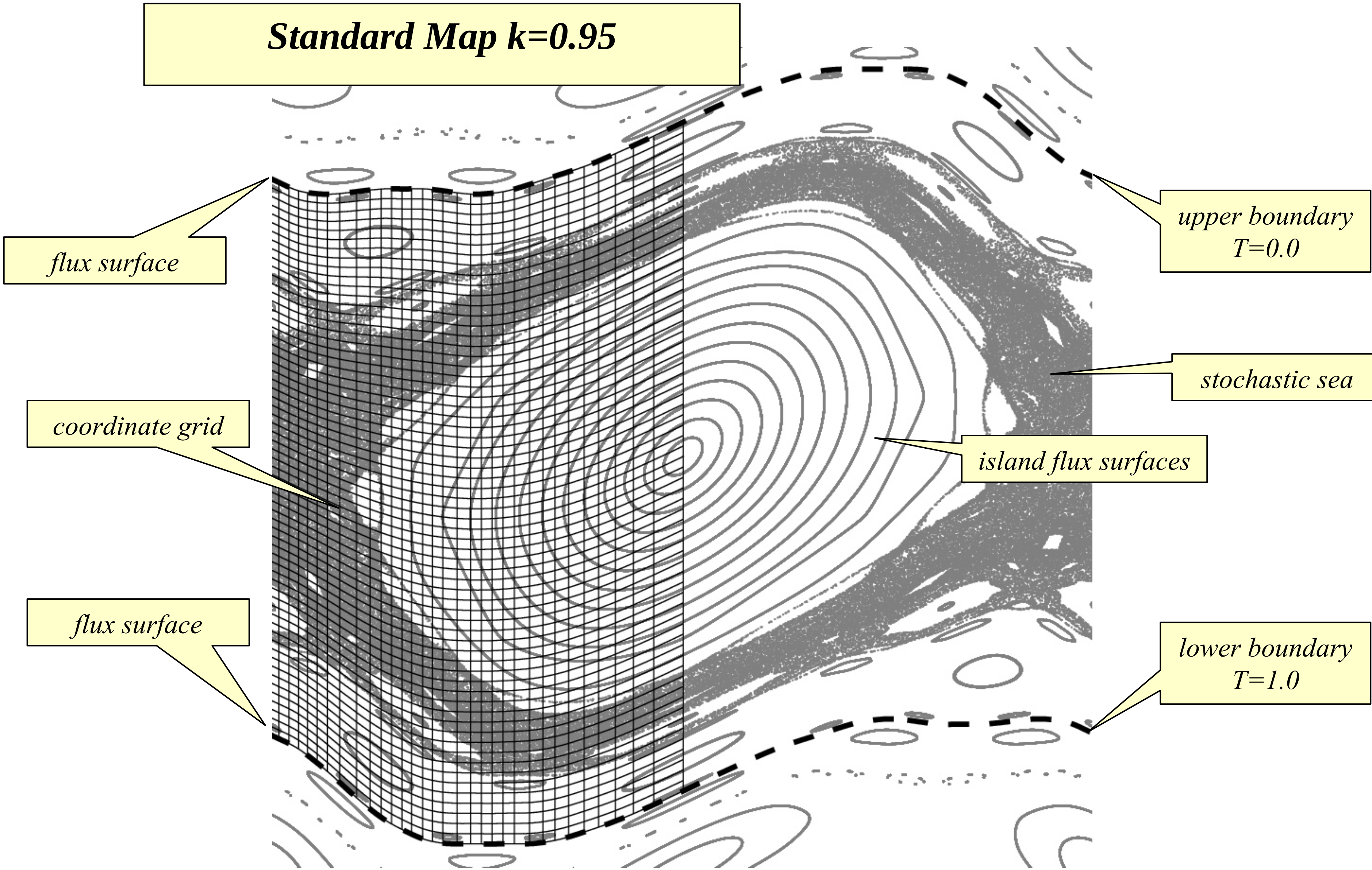

Steady state T contours are shown; the unstable manifold has an important effect

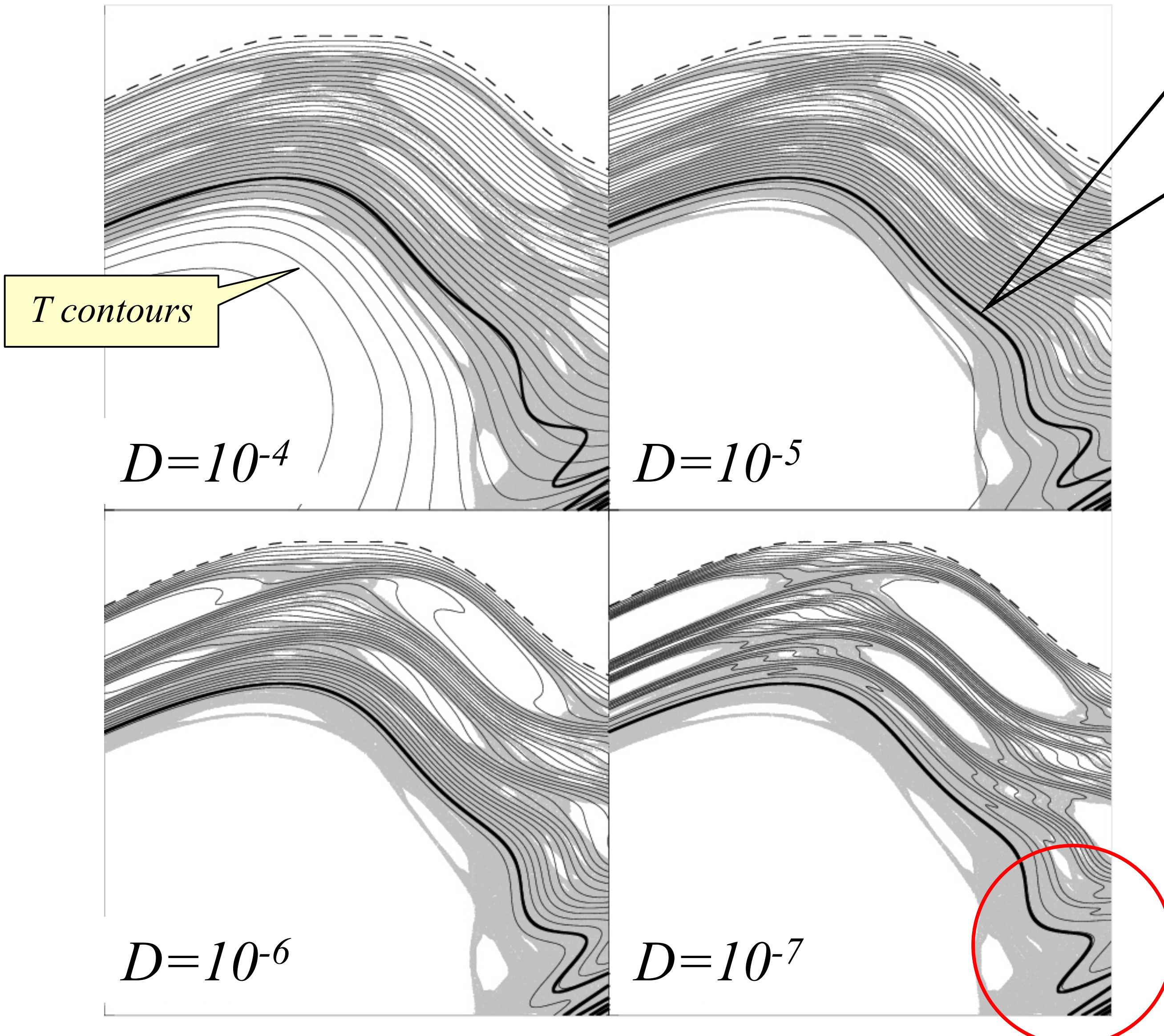

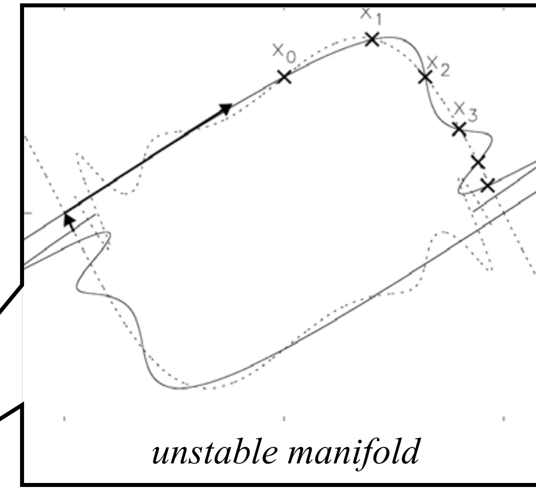

- *the importance of the unstable manifold is well known in fluid mechanics*
- *observed in DIIID heat footprint*
- *as D decreases, invariant manifolds play an important role*

The cantori have an important effect on advective-*diffusive* transport

cantori shown as black dots

T contours shown as lines

as D decreases, correlation between cantori and T improves

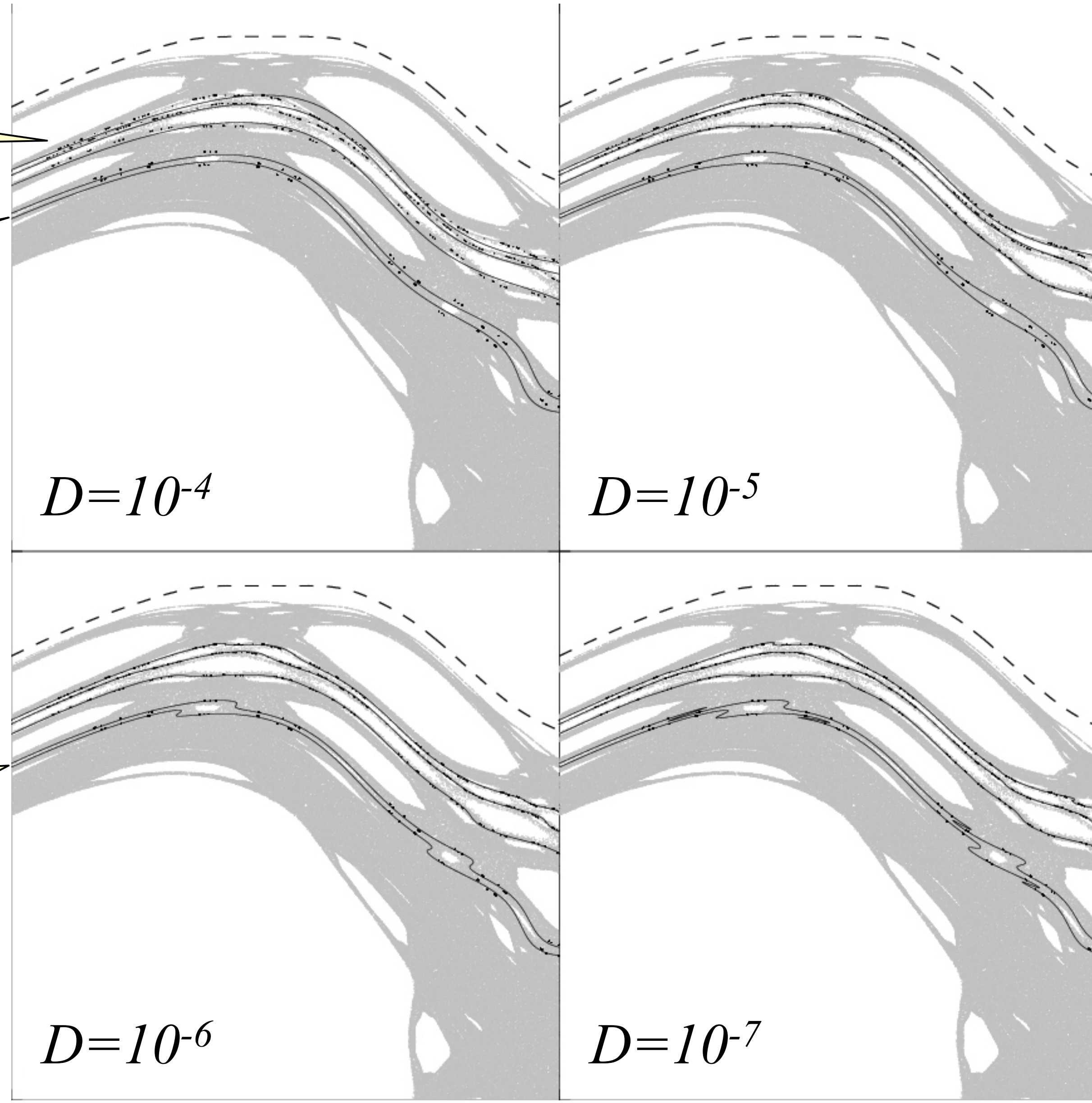

Ghostcurves fill in the holes in the cantori, and align with Temperature contours

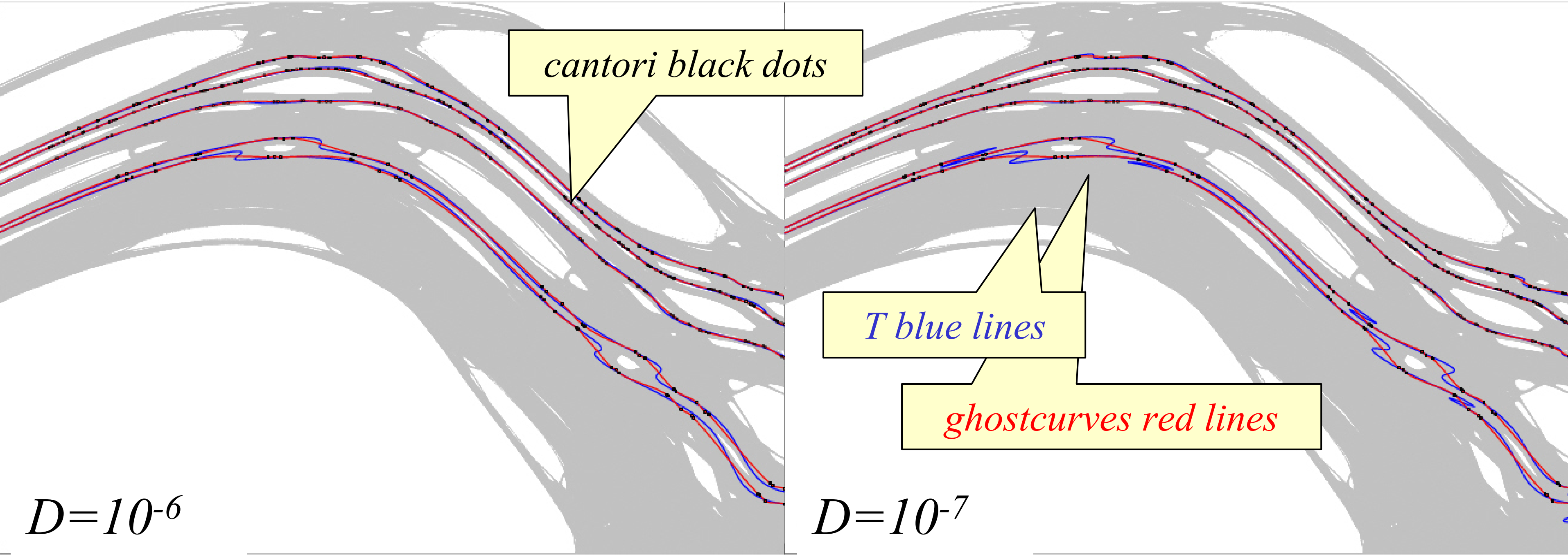

- *the "holes" in cantori are filled by ghostcurves,*
- *T contours, cantori and ghostcurves are related*

- depending on Diffusion, and criticality of cantorus

irrational : cantorus : ghost curve

[0,3,3,1,.]	521/1707	11/36
[0,3,2,1,.]	377/1275	13/44
[0,3,1,1,.]	233/843	21/76
[0,4,2,1,.]	610/2673	13/57
[0,4,1,1,.]	377/1741	13/60

Ghostcurves do not intersect, and may be used to form a chaotic coordinate grid

- *different ghostcurves don't intersect*
  - *interpolation might be problematic*
    -- careful selection of (p,q) required
- *can construct "chaotic-coordinates"*
  - *coordinates cannot straighten chaos,*
    -- but coordinates that capture the invariant periodic sets come close
- *a theory of diffusive-transport across ghostcurves may complement numerical work*

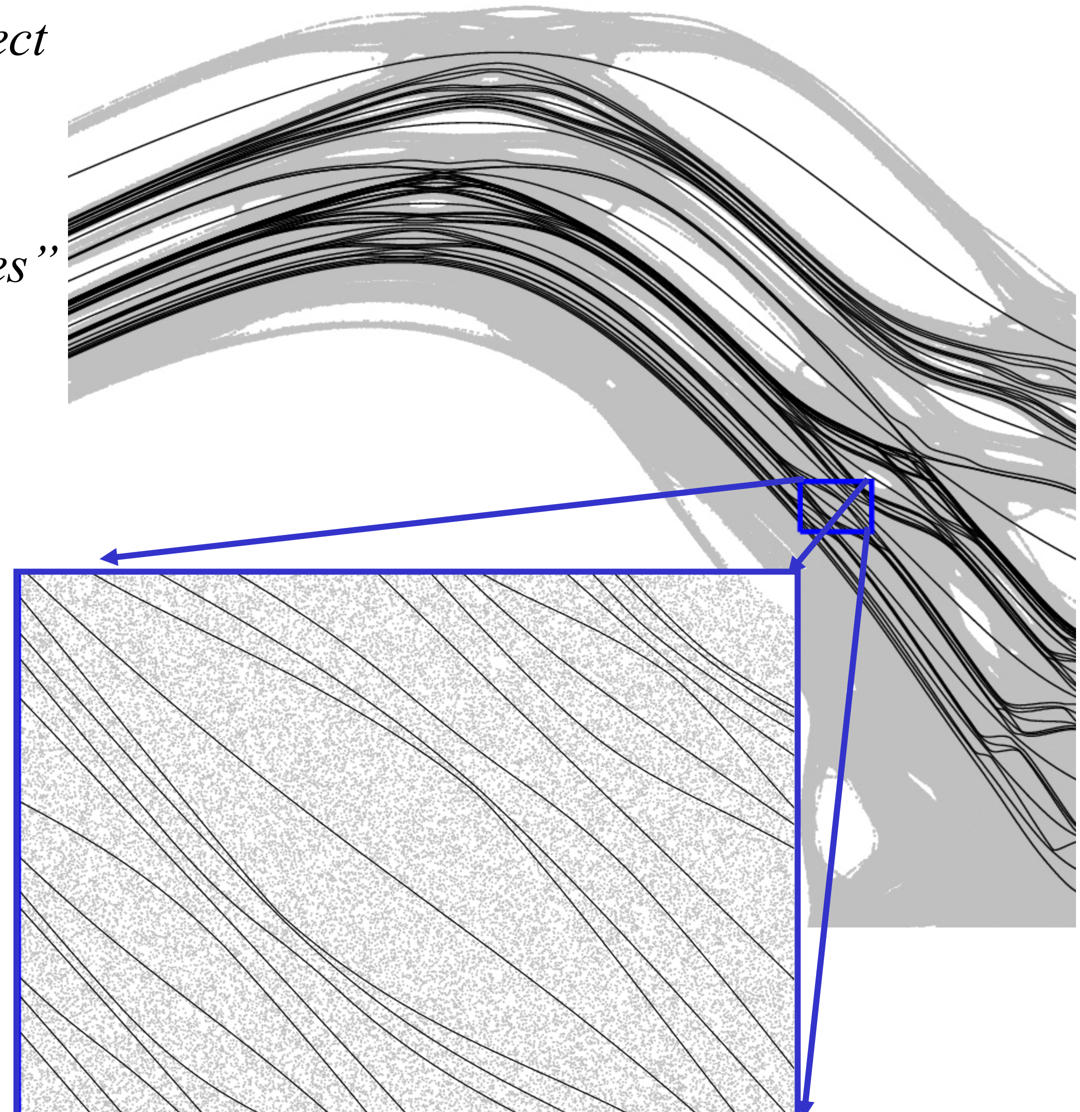

Further analysis is pending . . .

- Cantori, and other invariant sets such as the unstable manifold, clearly affect transport in chaotic, diffusive systems.
- Present work has given graphical evidence that shows cantori and *T* coincide, for small *D*
- Remains to quantify . . . .
  - degree of correlation between cantori and *T* (depends on degree of criticality, *D)*
  - what is the diffusive flux across the ghostcurves ? (depends on *D,* boundary conditions)
  - can constructing a set of cantori/unstable-manifolds/ghostcurves (fast) provide
    - a better initial guess for iterative solution of the steady-state Temperature ?
    - optimal coordinates for analysis of chaotic flows ?
- Plan to extend to consider heat-diffusion in chaotic fields

- extend to 3D, examine heat diffusion $q = -\kappa_{\parallel} \nabla_{\parallel} T - \kappa_{\perp} \nabla_{\perp} T$ in M3D

- examine transition from clean separatrix, with critical island width $W_c \propto \left(\kappa_{\perp} / \kappa_{\parallel} \right)^{1/4}$, to strongly chaotic case

Poincare recurrence